Fracture Properties and Toughening Mechanisms of Biodegradable Poly(L-lactic acid)/Poly(ε-caprolactone) Polymer Blend

Mitsugu Todo[*]

Research Institute for Applied Mechanics, Kyushu University, Kasuga, Fukuoka 816-8580, Japan

Abstract: PLLA/PCL polymer blends with different PCL contents were fabricated to examine the effect of PCL content on the bending mechanical properties of the blend. Three-point bending tests of beam specimens 5 mm thick were performed at both quasi-static and impact loading-rates, and then bending mechanical properties such as bending modulus, strength and fracture absorbed energy were evaluated. It was found that the modulus and strength decreased as PCL content increased, while the fracture absorbed energy tended to increase with increase of PCL content and was optimized with 15% PCL. Scanning electron microscopy of fracture surfaces and polarizing optical microscopy of tensile damage regions were also carried out to investigate the fracture mechanism of PLLA/PCL blend. It was found that the primary mechanisms involved in the bending fracture of PLLA/PCL blend were initiation of dense craze-like damage and following ductile deformation of the matrix. The model I fracture properties of PLLA/PCL were also evaluated and compared with those of pure PLLA. It was found that the fracture properties were dramatically improved by PCL blending and the primary toughening mechanisms were the aggregation formation of craze-like micro-damages in the process-zone with rough formation of fracture surface.

Keywords: Bioabsorbable polymer, Polymer blend, Ductile Fracture, Fracture energy absorption.

1. INTRODUCTION

A biodegradable aliphatic polyester poly(L-lactic acid) (PLLA) having higher L-lactide content in the polymeric group of poly(lactic acid) (PLA) have successfully been used as bone fixation devices in orthopedic and oral surgeries because of its absorbability and non-toxicity after degradation [1-5]. However, fracture problems of such PLLA implants have often been reported, and therefore, it is important to characterize the fracture behavior of PLLA and furthermore, it is an essential issue to improve its fracture resistance. The author's research group has extensively been studied the fracture properties and mechanism of PLLA, and characterized the effects of microstructure on the macroscopic fracture properties [6-9].

On the other hand, it is well-known that one of the effective ways to improve the fracture properties of a brittle polymer is physical blending with a ductile polymer [10]. Poly(ε-caprolactone) (PCL) is another degradable aliphatic polyester which is also bioabsorbable and biocompatible and in rubbery state at room temperature with Tg around -60°C. Physical blending of PLA with PCL was firstly investigated by Tsuji and Ikada [11,12], and they showed that a PLLA/PCL blend with PCL content of 25wt% has much larger fracture strain with small reduction of strength than PLLA. Since then, many works have been conducted to understand the microstructures and mechanical properties of PLA/PCL blends [13-24]. For example, nanoparticles were mixed with PLA/PCL to improve the mechanical properties [18,19,23]. Most of these works were, however, conducted using thin film samples fabricated by solution-cast blending, although plates of about 2mm thick are usually used for bioabsorbable bone fixation devices. It is therefore important to understand the fracture behavior of such thick samples of polymer blends.

The aim of the present study is to characterize the fracture properties and the fracture mechanisms of thick plate samples of PLLA/PCL blends. A conventional melt mixing technique was utilized to obtain blends of PLLA and PCL, and a hot-press was used to fabricate thick plate specimens. Mechanical bending properties were then evaluated by three-point bending tests under static and impact loadings, and effects of PCL content on the bending mechanical properties were examined. Fracture micromechanism was also investigated by polarizing optical microscopy and field emission scanning electron microscopy, and correlated with the macroscopic bending fracture properties.

2. EXPERIMENTAL

2.1. Materials and Specimens

PLLA pellets were provided from Shimadzu Co., Ltd. The weight average molecular weight M_w, the glass transition temperature T_g and the melting point

*Address correspondence to this author at the Research Institute for Applied Mechanics, Kyushu University, 6-1 Kasuga-koen, Kasuga, Fukuoka 816-8580, Japan; Tel: +81-92-583-7762; Fax: +81-92-583-7763;
E-mail: todo@riam.kyushu-u.ac.jp

T_m of the pellets are 200,000gmol^{-1}, 60.7°C and 172.6°C, respectively. PCL pellets were provided by Daicel Chemistries Ltd. M_w, T_g and T_m are 70,000gmol^{-1}, -40°C and 60°C, respectively. PLLA and PCL pellets were blended using a conventional melt mixing machine for one hour at 180°C and at a rotor speed of 100 rpm. The mixing ratios chosen were PLLA/PCL=95/5, 90/10, 85/15 and 80/20 in weight fraction. These blends are simply denoted, for example, as PLLA/PCL5 where 5 is the PCL content thereafter. Pellets of PLLA/PCL blends were prepared from the mixture, and plates of 60 x 60 x 5 mm^3 were fabricated from these pellets using a hot-press at 180°C under 30MPa. Beam specimens of 60 x 10 x 5 mm^3 were then processed from these plates. Neat PLLA specimens were also fabricated for comparison. Single-edge-notched beam (SENB) specimens were prepared from some of these beam specimens by introducing notches by machining. The geometries of the three-point bending and the single-edge-notched-bend (SENB) specimens are shown in Figure **1**.

(a) Three-point bending specimen

(b) Single-edge-notched-bend specimen
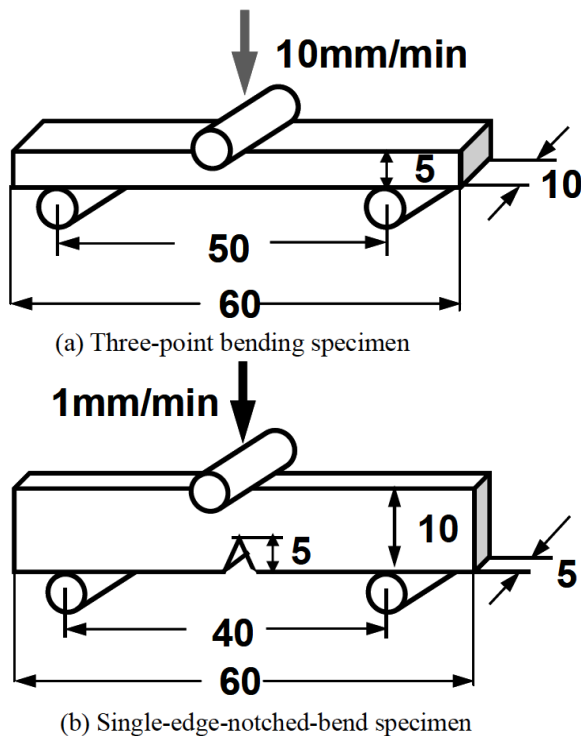
Figure 1: Microstructure of PLLA/PCL15.

2.2. Measurements of Bending Mechanical and Mode I Fracture Properties

Quasi-static three-point bending tests were performed using the three-point bending specimen (Figure **1a**) to evaluate bending mechanical properties at a loading-rate of 10mm/min using a servohydraulic testing machine. The span length was 50mm. Load-

displacement (P-δ) curves were recorded using a digital recorder. Bending modulus, E, and bending strength, σ_f, and fracture absorbed energy, U_f, were then evaluated using the following formulas:

$$E = \frac{L^3}{4DH^3} S \tag{1}$$

$$\sigma_f = \frac{3P_{max}L}{2DH^2} \tag{2}$$

$$U_f = \frac{1}{A_0} \int_0^{\delta_f} Pd\delta \tag{3}$$

where L is the span length, and D and H are the width and thickness of the specimen, respectively. S is the initial slope of load-displacement curve. P_{max} is the maximum load. A_0 is the initial cross-sectional area, and δ_f the displacement at fracture.

Impact three-point bending tests were also carried out using the same specimen shown in Figure **1a** to obtain impact bending properties at a loading-rate of 1m/s using an instrumented drop weight testing system. In this system, load is measured by piezo-electric load-cell attached to the loading dart, and loading-point displacement is directly measured with use of a dynamic displacement measuring apparatus consisting of optical fiber, laser, position sensing detector and operation amplifier [10-12]. The impact testing system is schematically shown in Figure **2**. Bending modulus, strength and fracture absorbed energy were then estimated using eqs. (1)-(3) from the load-displacement curves obtained.
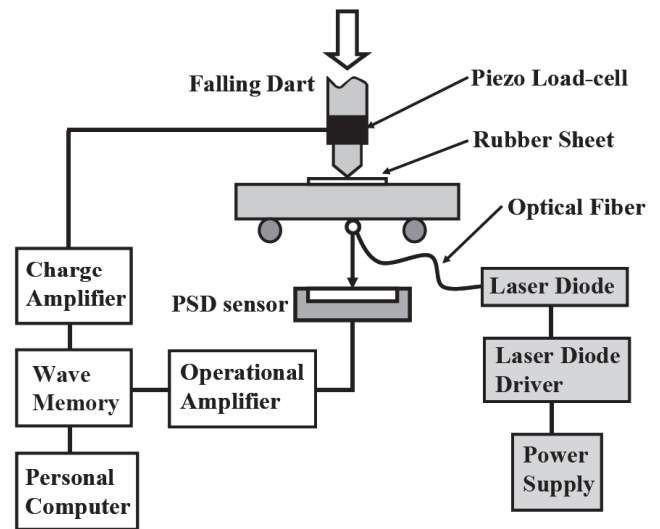
Figure 2: Schematic of drop weight impact testing system.

Mode I fracture properties, the critical stress intensity factor K_{IC} and the critical energy release rate

G_{IC} were also evaluated using the SENB specimen shown in Figure **1b** for neat PLLA and PLLA/PCL15 blend using the following formula:

$$K_{IC} = f \frac{P_C}{B\sqrt{W}} \tag{4}$$

$$G_{IC} = \frac{U_C}{BW\phi} \tag{5}$$

where P_C and is U_c are the critical load and the critical energy, respectively. B and W are the thickness and the width of the SENB specimens, respectively, and f and ϕ are the geometrical correction factors given by functions of a/W where a is the initial crack length.

2.3. Microscopy

Thin samples were prepared from PLLA and PLLA/PCL15 specimens for polarizing optical microscopy (POM) of damage formation. For the beam and SENB specimens, applied load was stopped at maximum, and thin samples of the damaged regions were prepared using the thin sectioning technique [13]. Scanning electron microscopy (SEM) of fracture surfaces created under quasi-static and impact loadings was also performed using a field emission scanning electron microscope to assess the effect of loading rate on fracture surface morphology.

3. RESULTS AND DISCUSSION

3.1. Bending Mechanical Properties

Load-displacement curves obtained at the quasi-static rate of 10mm/min are shown in Figure **3**. PLLA and PLLA/PCL5 exhibited sudden decrease of load just
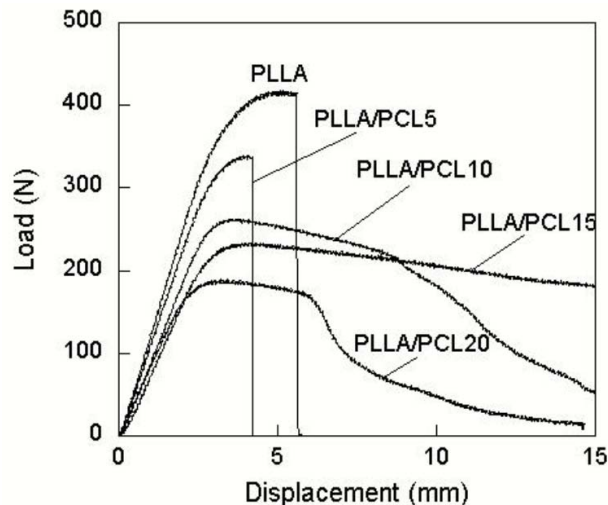
Figure 3: Static load-displacement curves.

after the peak point of load corresponding to brittle fracture behavior; on the contrary, the other PLLA/PCL blends showed ductile fracture behavior with slow decrease of load after the peaks, suggesting that the fracture behavior is changed from brittle to ductile manner with increase of PCL content. It is noted that the reduction rate of load in PLLA/PCL15 after maximum was the slowest of the three blends, suggesting its fracture energy dissipated by damage formation may be the largest. The detail of the mechanism of the slowest reduction rate of PLLA/PCL15 is discussed in the following section.

Static bending properties are shown as a function of PCL content in Figure **4**. Bending modulus and strength decreased as PCL content increased due to lower modulus and strength of PCL than PLLA. However, fracture absorbed energy exhibited a different behavior and was maximized at 15wt%, suggesting that structural optimization was achieved at this blend ratio.

Impact fracture properties of only PLLA/PCL15 were measured and compared with those of neat PLLA because the static fracture absorbed energy of the blend was the highest as shown in Figure **4c**. Results of such comparison are shown in Figure **5**. For both PLLA and PLLA/PCL15, the impact modulus was little higher than the static one. The impact strength of PLLA was slightly higher than the static one; on the other hand, the impact strength of PLLA/PCL15 is 30% higher than the static one. As a result, the difference of the impact strength between PLLA and PLLA/PCL15 became smaller. The impact absorbed energy of PLLA/PCL15 was 2 times higher than that of PLLA. Thus, the fracture absorbed energy of PLLA under static and impact bending can be improved by blending PCL and is optimized with 15wt% PCL.

3.2. Bending Failure Mechanism

POM micrographs of the tensile-stress regions of the three-point bending specimens are shown in Figure **6**. For the neat PLLA, many straight crazes are observed in the direction parallel to the loading direction and also perpendicular to the tensile direction. These crazes are transformed to cracks when the molecule bundles connecting the surfaces of the crazes are broken off and then brittle fracture occurs, corresponding to the sudden drop appeared on the load-displacement curve shown in Figure **3**. On the contrary, PLLA/PCL15 exhibits dense curved craze-like damages and the damages seem to cross each other. This type of damage may not be easily transformed to

(a) Bending modulus

(b) Bending strength

(c) Fracture absorbed energy
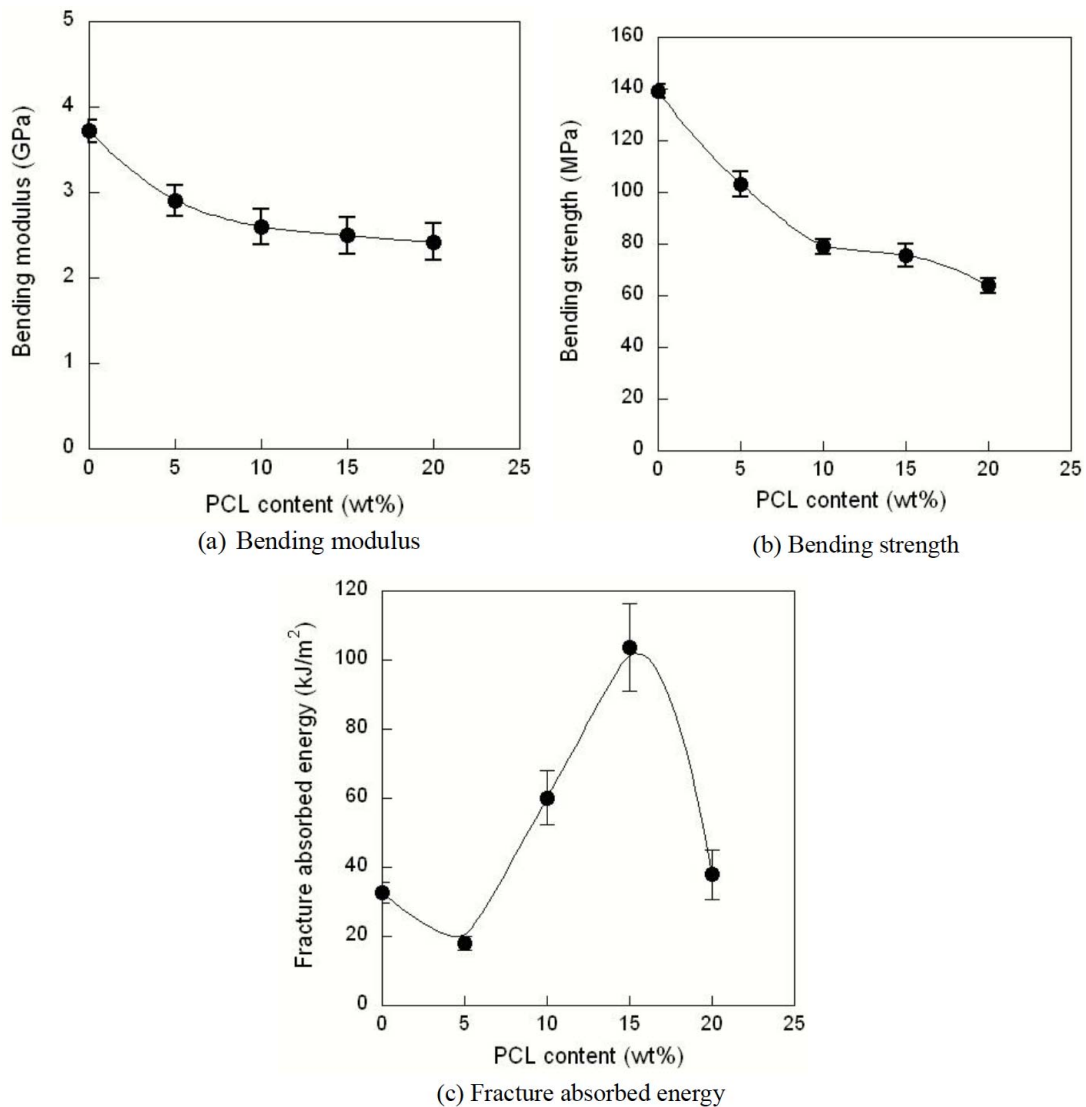
Figure 4: Effects of PCL content on static bending properties.

a crack and prevent brittle fracture. Therefore, larger energy is dissipated during such damage formation than the combined failure of crazing and brittle crack propagation in neat PLLA. The fracture surfaces of four different blends obtained at the static loading rate are compared in Figure **7**. It is clearly seen that the ductility of the surface was most significant in PLLA/PCL15 with elongated fibrils. The other surfaces indicated relatively smooth morphology compared to PLLA/PCL15. It is therefore thought that the generation of such ductile fibril structures resulted in the slowest reduction rate of load-displacement curve shown in Figure **3**. SEM micrographs of bending fracture surfaces of PLLA and PLLA/PCL15 are shown in Figure **8**. It is obviously seen that PLLA showed smooth fracture surfaces corresponding to low fracture absorbed energy shown in Figure **5c**. On the other hand, PLLA/PCL15 showed very ductile fracture surface with elongated fibrils under static loading and the surface became relatively flat

and smooth under impact loading but still rougher than the fracture surfaces of PLLA. These fracture surface morphology well corresponds to Figure **5c** in which the impact energy of PLLA/PCL15 was much lower than the static energy and still higher than the impact energy of PLLA.

Failure mechanism of PLLA/PCL15 under bending load condition is discussed on the basis of Figure **9** in detail. The fracture of a PLLA/PCL15 bend specimen is initiated by formation of a crack in the tensile stress region as shown in Figure **9a**. In this region, as tensile stress increases, the stress concentration in the surroundings of a PCL spherulite also increases and then, a void is formed due to the interfacial failure at the PCL-PLLA interface as shown in Figure **9b**. A colsence of the voids becomes a craze-like damage as shown in Figure **9c**. The craze-like damage finally grows up to the crack accompanied by scission of the PLLA fibrils.

(a) Bending modulus

(b) Bending strength

(c) Fracture absorbed energy
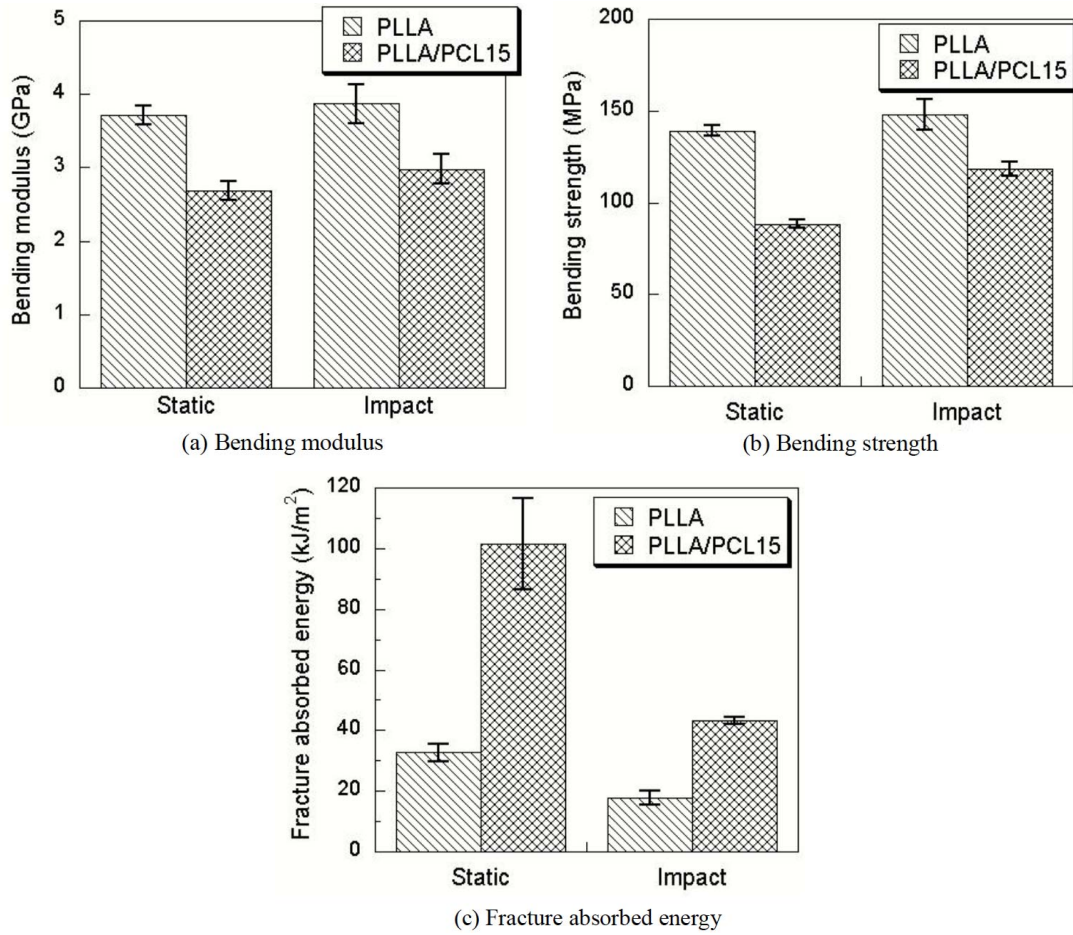
Figure 5: Comparison of PLLA and PLLA/PCL15 on static and impact properties.

(a) PLLA
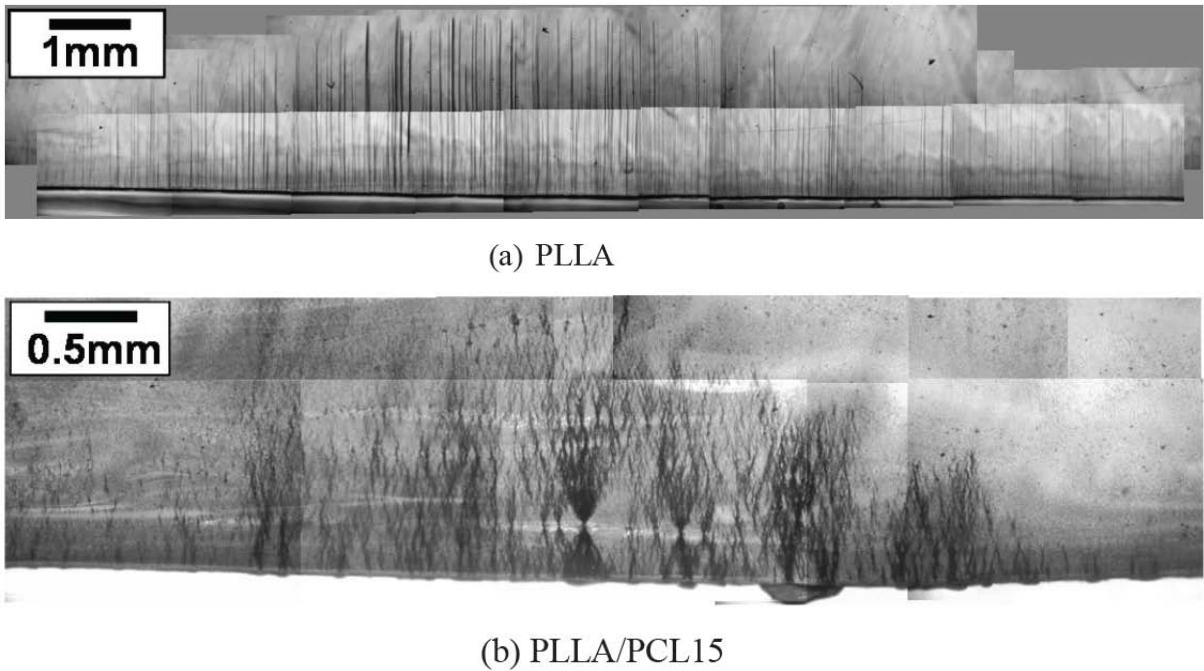
(b) PLLA/PCL15

Figure 6: Damage formations in tensile-stress regions under three-point bending.

(a) PLLA/PCL5   (b) PLLA/PCL10

(c) PLLA/PCL15   (d) PLLA/PCL20
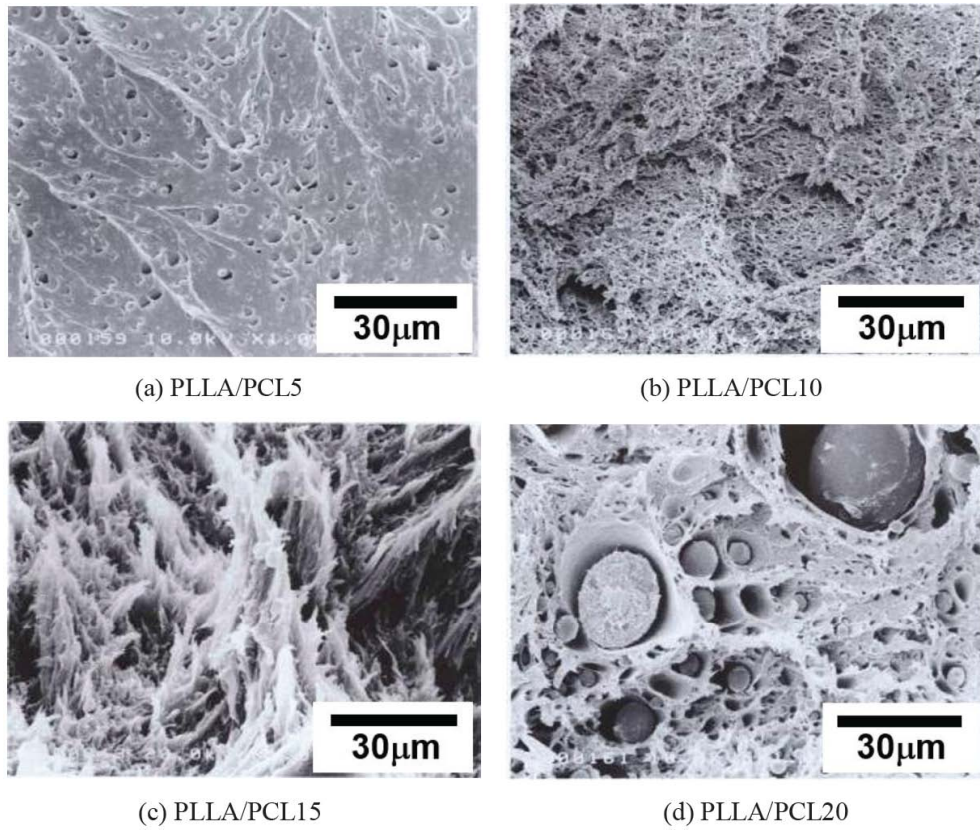
Figure 7: SEM micrographs of bending fracture surfaces.

(a) PLLA, static   (b) PLLA, impact

(c) PLLA/PCL15, static   (d) PLLA/PCL15, impact
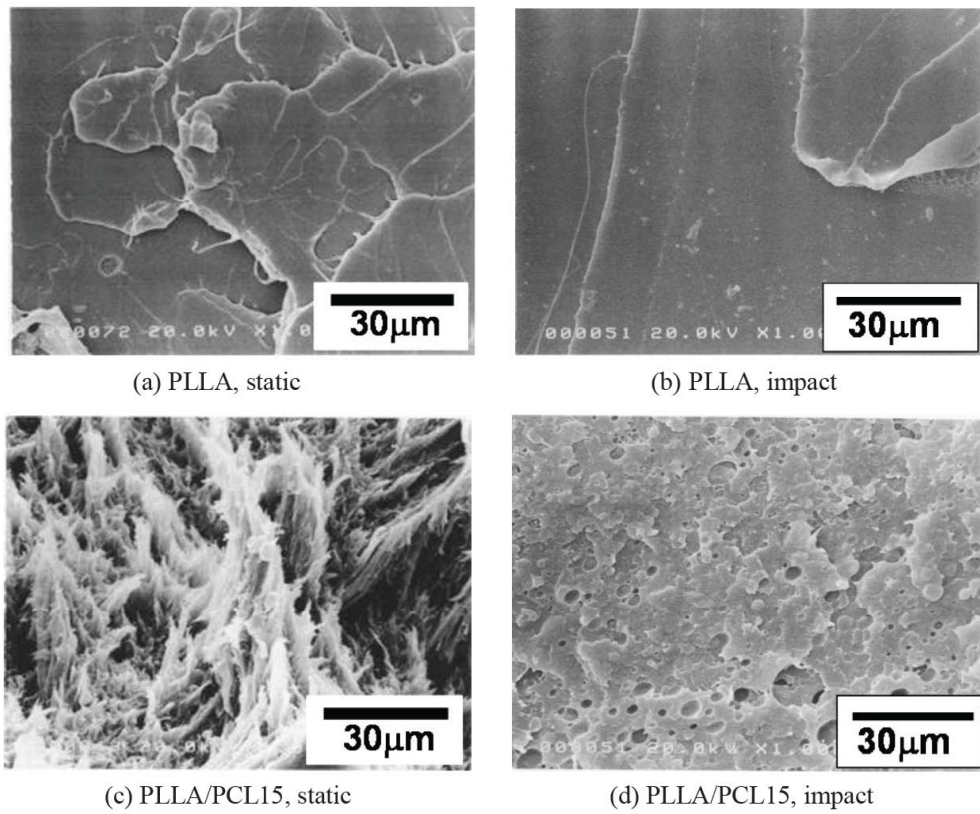
Figure 8: Comparison of bending fracture surfaces of PLLA and PLLA/PCL15.

(a) Failure behavior in the tensile stress region

(b) Void formation with a PCL spherulite

(c) Craze-like damage formation

(d) Elongated fibrils with PCL spherulites
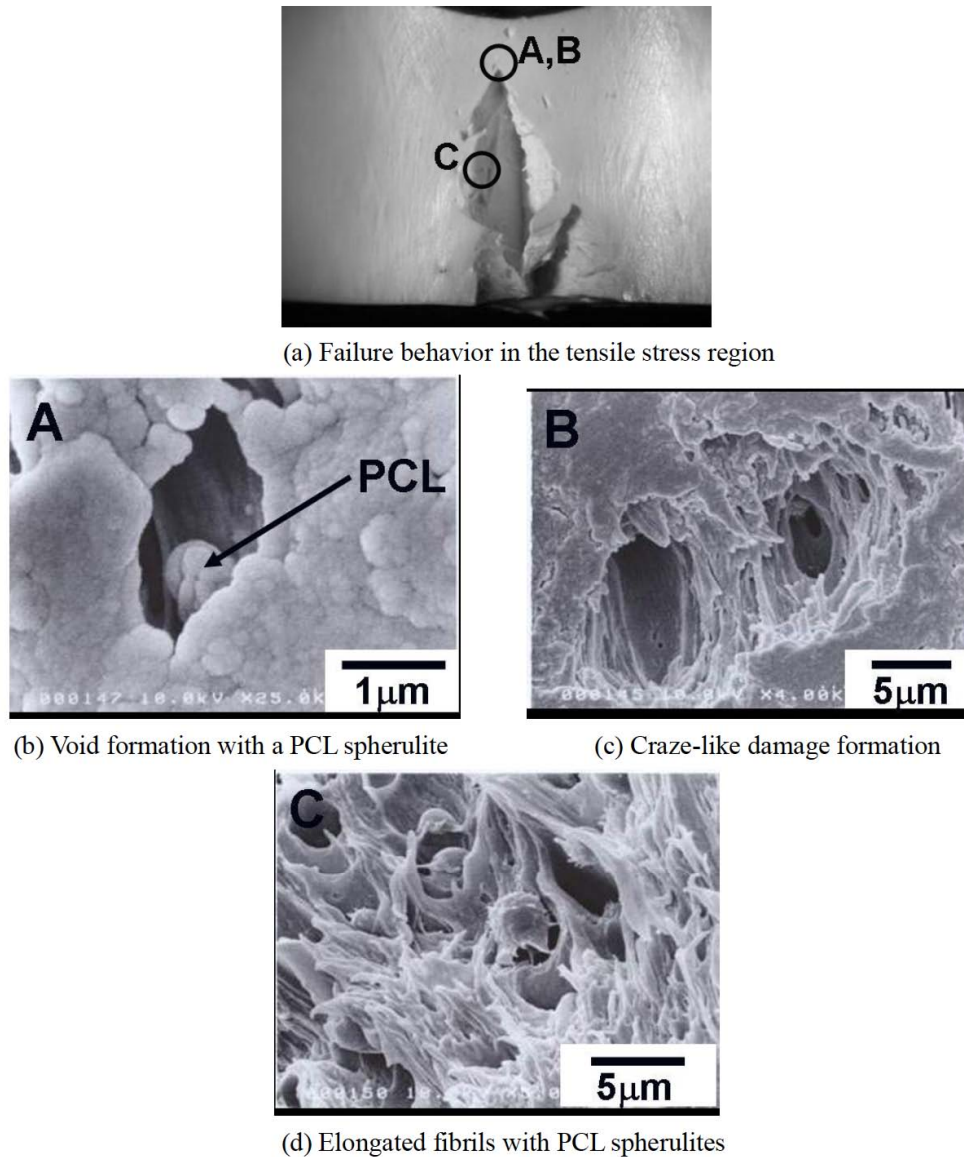
Figure 9: Micro-damage formation in PLLA/PCL15 under three-point bending.

3.3. Mode I Fracture Properties

Typical load-displacement curves obtained from mode I fracture tests are shown in Figure **10**. The maximum load of PLLA is slightly higher than PLLA/PCL15 but the corresponding displacement is much lower. PLLA shows sudden decrease of load after the maximum load indicating rapid crack grown behavior; on the contrary, PLLA/PCL15 shows slowly decreasing load corresponding to slow crack growth behavior. Mode I fracture properties, K_{IC} and G_{IC}, are shown in Figure **11**. K_{IC} of PLLA/PCL15 is slightly smaller than that of PLLA, while G_{IC} of the blend is about twice as much as that of PLLA. This indicates that fracture energy can be improved by blending PCL with PLLA; however, stress-based fracture criterion tends to decrease due to the blending.
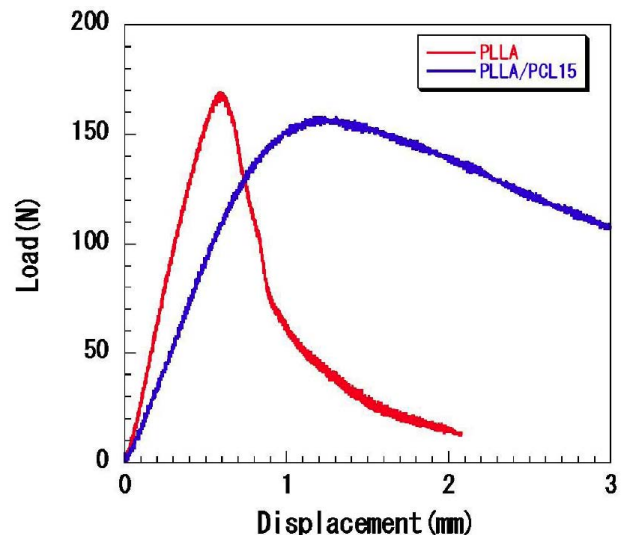
Figure 10: Load-displacement curves obtained from mode I fracture tests.
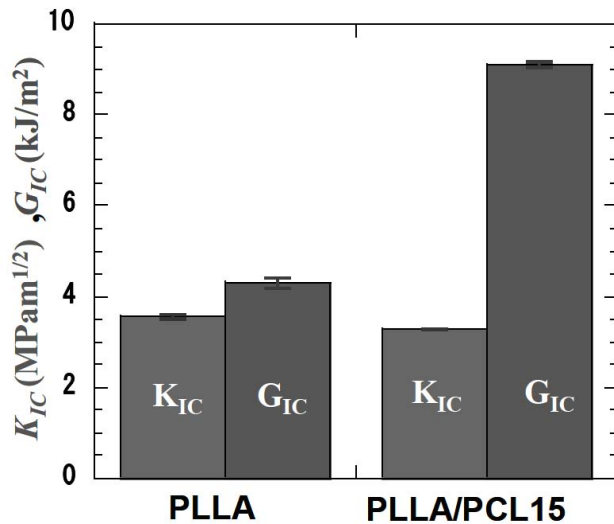
Figure 11: Mode I fracture properties.

3.4. Mode I Fracture Mechanism

POM micrographs of the damage formation in the crack-tip regions, so called 'process-zone', are shown in Figure **12**. Multiple craze formation is observed in PLLA, while a cloud of fine damages are formed in PLLA/PCL15. SEM micrographs of the damages in the process-zone are shown in Figure **13**. It is clearly seen that the damages formed craze-like micro-structures connecting the upper and bottom crack surfaces by micro-fibrils. Similar micro-damages were also observed in our previous research [24]. Typical fracture surfaces of PLLA and PLA/PCL15 under mode I fracture are also shown in Figure **14**. It is observed that the surface of the blend is much rougher than that of PLLA, suggesting more energy dissipation due to the ductile elongation and breakage of polymer fibrils during the crack propagation process. These aggregation formation of micro-damages tend to dissipate more energy than the several lines of single craze appeared in PLLA, resulting in the improvement of G_{IC}, and also reduce the stress intensity in the crack-tip region, resulting in the increase of K_{IC}, as shown in Figure **11**. Thus, the improvement of the fracture properties, K_{IC} and G_{IC}, observed in the polymer blend are closely related to the micro-damage formation in the process-zone under the crack-tip stress concentration.

4. CONCLUSIONS

Fracture properties and toughening mechanisms of biodegradable PLLA/PCL polymer blend were characterized under the deformation modes of three-point bending and mode I fracture. Static and impact three-point bending tests and mode I fracture tests using SENB specimens were performed to evaluate the bending mechanical properties and mode I fracture properties of PLLA and PLLA/PCL blends. Optical and

(a) PLLA

(b) PLLA/PCL15

Figure 12: Damage formation in the crack-tip regions of SENB specimens.
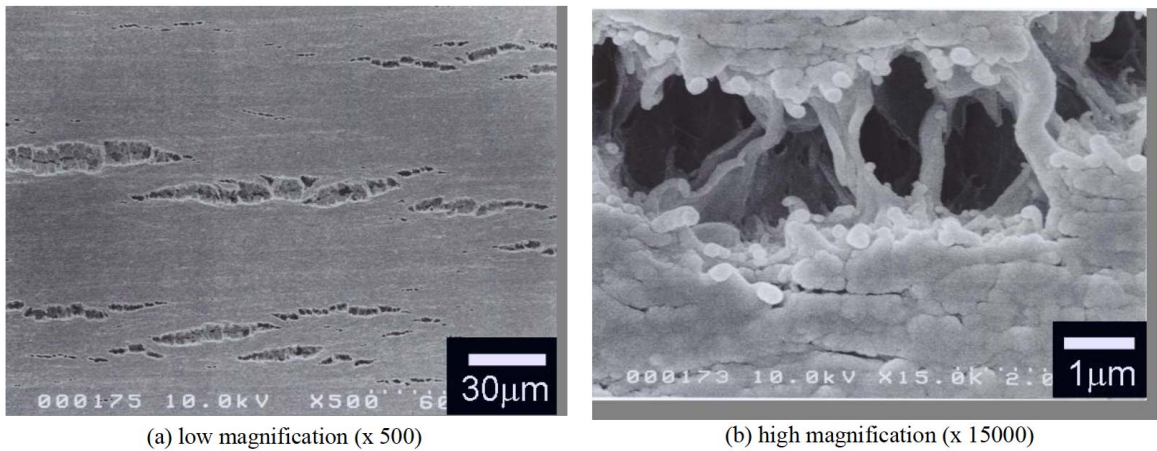
(a) low magnification (x 500)   (b) high magnification (x 15000)

Figure 13: Formation of craze-like damage in the process zone of PLLA/PCL15.
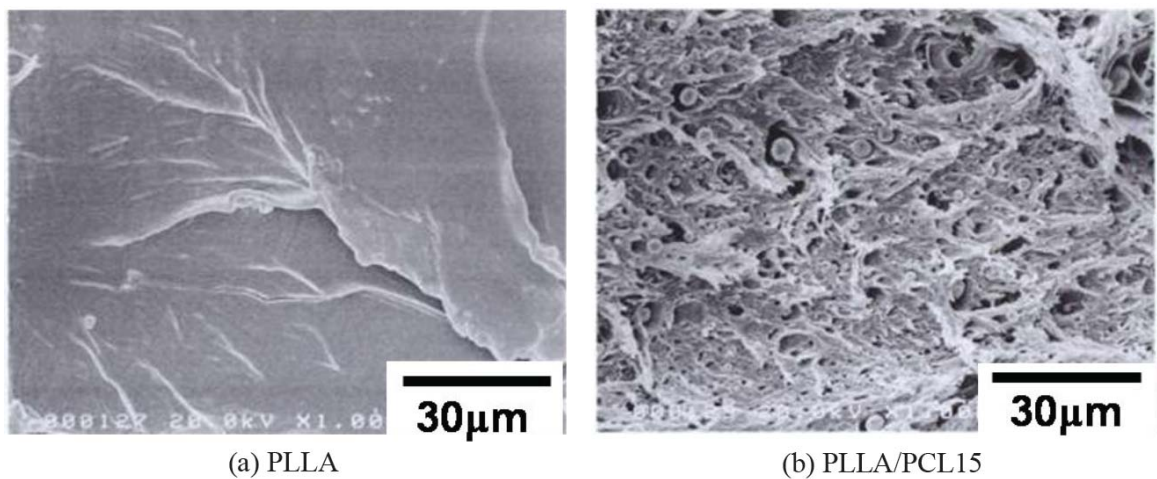
(a) PLLA   (b) PLLA/PCL15

Figure 14: SEM micrographs of mode I fracture surfaces.

scanning electron microscopies were also conducted to characterize the fracture micro-mechanisms. The conclusions were obtained as follows:

1. For PLLA/PCL blend, static bending modulus and strength decreased as PCL content increased. Static fracture absorbed energy is however improved by blending, and the energy value is maximized at 15wt% of PCL. Static fracture absorbed energy of PLLA/PCL15 is 3.5 times larger than that of neat PLLA.

2. Impact fracture absorbed energy of PLLA/PCL15 was about 2 times higher than that of neat PLLA. Thus, the fracture absorbed energy of PLLA can be improved by blending with PCL under both static and impact loading conditions.

3. In PLLA, formation of multiple straight crazes was the primary mechanism of bending fracture, while in PLLA/PCL, dense curved craze-like damages were formed in the tensile stress region. This type of damage did not easily change to crack, as a result, much higher energy was dissipated during the fracture process than in neat PLLA. Rough surfaces indicating ductile deformation and fracture of fibril structures were also observed on the fracture surfaces, suggesting the higher energy dissipation on the surface regions.

4. Mode I fracture properties such as KIC and GIC of PLLA/PCL15 were found to be much higher than those of neat PLLA. These improvement of the fracture properties were also caused by the aggregation formation of multiple craze-like micro-damages in the process-zone with creation of rough fracture surface.

REFERENCES

[1] Higashi S, Tamamoto T, Nakamura T, Ikada Y, Hyon SH, Jamshidi K. Polymer-hydroxyapatite composites for biodegradable bone fillers. Biomaterials 1986; 7(3): 183-187. https://doi.org/10.1016/0142-9612(86)90099-2

[2]   Ikada Y, Shikinami Y, Hara Y, Tagawa M, Fukada E. Enhancement of bone formation by drawn poly(L-lactide). Journal of Biomedical Materials Research 1996; 30(4): 553-558.
https://doi.org/10.1002/(SICI)1097-4636(199604)30:4<553::AID-JBM14>3.0.CO;2-I

[3]   Mohanty AK, Misra M, Hinrichsen G. Macromol Mater Eng 2000; 276/277: 1.
https://doi.org/10.1002/(SICI)1439-2054(20000301)276:1<1::AID-MAME1>3.0.CO;2-W

[4]   Shafer BL, Simonian PT. Broken poly-L-lactic acid interference screw after ligament reconstruction. Arthroscopy 2002; 18(7): E35.
https://doi.org/10.1053/jars.2002.32197

[5]   Kosaka M, Uemura F, Tomemori S, Kamiishi H. Scanning electron microscopic observations of 'fractured' biodegradable plates and screws. Journal of Cranio-Maxillofacial Surgery 2003; 31(1): 10-14.
https://doi.org/10.1016/S1010-5182(02)00166-X

[6]   Todo M, Shinohara N, Arakawa K. Effects of Crystallization and Loading-rate on the Mode I Fracture Toughness of Biodegradable Poly(lactic acid). Journal of Materials Science Letters 2002; 21: 1203-1206.
https://doi.org/10.1023/A:1016520518959

[7]   Park SD, Todo M, Arakawa K. Effect of Annealing on the Fracture Toughness of Poly(lactic acid). Journal of Materials Science 2004; 39: 1113-1116.
https://doi.org/10.1023/B:JMSC.0000012957.02434.1e

[8]   Park SD, Todo M, Arakawa K. Effect of annealing on fracture mechanism of biodegradable poly(lactic acid). Key Engineering Materials 2004; 261-263: 105-110.
https://doi.org/10.4028/www.scientific.net/KEM.261-263.105

[9]   Park SD, Todo M, Arakawa K, Koganemaru M. Effect of crystallinity and loading-rate on mode I fracture behavior of poly(lactic acid). Polymer 2006; 47: 1357-1363.
https://doi.org/10.1016/j.polymer.2005.12.046

[10] Todo M, Takahashi J, Watanabe H, Nakamoto J, Arakawa K. Effect of Loading-rate on fracture micromechanism of methylemethacrylate-butadiene-styrene polymer blend. Polymer 2006; 47: 4824.
https://doi.org/10.1016/j.polymer.2006.04.042

[11] Tsuji H, Ikada Y. Blends of aliphatic polyesters. I. Physical properties and morphologies of solution-cast blends from poly(DL-lactide) and poly(ε-caprolactone). Journal of Applied Polymer Science 1996; 60(13): 2367-2375.
https://doi.org/10.1002/(SICI)1097-4628(19960627)60:13<2367::AID-APP8>3.0.CO;2-C

[12] Tsuji H, Ikada Y. Blends of aliphatic polyesters. II. Hydrolysis of solution-cast blends from poly(L-lactide) and poly(ε-caprolactone) in phosphate-buffered solution. Journal of Applied Polymer Science 1998; 67(3): 405-415.
https://doi.org/10.1002/(SICI)1097-4628(19980118)67:3<405::AID-APP3>3.0.CO;2-Q

[13] Broz ME, VanderHart DL, Washburn NR. Structure and mechanical properties of poly(D,L-lactide acid)/poly(epsilon-caprolactone) blends. Biomaterials 2003; 24(23): 4181-4190.
https://doi.org/10.1016/S0142-9612(03)00314-4

[14] Liangliang L, Defeng W, Ming Z, Weidong Z. Fabrication of polylactide/poly(ε-caprolactone) blend fibers by electrospinning: morphology and orientation. Indusgtrial & Engineering Chemistry Research 2012; 51(9): 3682-3691.
https://doi.org/10.1021/ie2028969

[15] Tatiana P, Antonio G, Paulo B. Mechanical and biological behaviour of PCL and PCL/PLA scaffolds for tissue engineering applications. Chemical Engineering Transactions 2013; 32: 1645-1650.

[16] Song ZJ, Huang XL, Lu XL, Lv QQ, Xu N, Pang SJ, Pan LS, Li T. Improvement of microstructures and properties of poly(lactic acid)/poly(ε-caprolactone) blends compatibilized with polyoxymethylene. Journal of Applied Polymer Science 2018; 135(31): 46536.
https://doi.org/10.1002/app.46536

[17] Botlhoko OJ, Ramontja J, Ray SS. A new insight into morphological, thermal, and mechanical properties of melt-processed polylactide/poly(ε-caprolactone) blends. Polymer Degradation and Stability 2018; 154: 84-95.
https://doi.org/10.1016/j.polymdegradstab.2018.05.025

[18] Kelnar I, Kratochvil J, Kapralkova L, Zhigunov A, Nevoralova M. Graphite nanoplatelets-modified PLA/PCL: Effect of blend ratio and nanofiller localization on structure and properties. Journal of the Mechanical Behaivor of Biomedical Materials 2017; 71: 271-278.
https://doi.org/10.1016/j.jmbbm.2017.03.028

[19] Urquijo J, Dagreou S, Guerrica-Echevarria G, Eguiazabal JI. Structure and properties of poly(lactic acid)/poly(ε-caprolactone) nanocomposites with kinetically induced nanoclay location. Journal of Applied Polymer Science 2016; 133(33): 43815.
https://doi.org/10.1002/app.43815

[20] Ferri JM, Fenollar O, Jorda-Vilaplana A, Garcia-Sanoguera D, Balart R. Effect of miscibility on mechanical and thermal properties of poly(lactic acid)/polycaprolactone blends. Polymer International 2016; 65(4): 453-463.
https://doi.org/10.1002/pi.5079

[21] Urquijo J, Guerrica-Echevarria G, Eguiazabal JI. Melt processed PLA/PCL blends: Effect of processing method on phase structure, morphology, and mechanical properties. Journal of Applied Polymer Science 2015; 132(41): 42641.
https://doi.org/10.1002/app.42641

[22] Gustafsson G, Nishida M, Ito Y, Haggblad HA, Jonsen P, Takayama T, Todo M. Mechanical characterization and modelling of the temperature-dependent impact behaviour of a biocompatible poly(L-lactide)/poly(ε-caprolactone) polymer blend. Journal of the Mechanical Behavior of Biomedical Materials 2015; 51: 279-290.
https://doi.org/10.1016/j.jmbbm.2015.07.007

[23] Agwuncha SC, Ray SS, Jayaramudu J, Khoathane C, Sadiku R. Influence of boehmite nanoparticle loading on the mechanical, thermal, and rheological properties of biodegradable polylactide/poly(ε-caprolactone) Blends. Macromolecular materials and Engineering 2015; 300(1): 31-47.
https://doi.org/10.1002/mame.201400212

[24] Todo M, Park SD, Takayama T, Arakawa K. Fracture micromechanisms of bioabsorbable PLLA/PCL polymer blends. Engineering Fracture Mechanics 2007; 74: 1872-1883.
https://doi.org/10.1016/j.engfracmech.2006.05.021